Shape- and orientation-dependence of surface barriers in single crystalline d-wave $Bi_2Sr_2CaCu_2O_{8+\delta}$

A.E. Böhmer, M. Konczykowski, C.J. van der Beek
Laboratoire des Solides Irradiés, CNRS-UMR 7642 & CEA/DSM/IRAMIS,
Ecole Polytechnique, F 91128 Palaiseau cedex, France
(Dated: April 29, 2010)

Magneto-optical imaging and Hall-probe array magnetometry are used to measure the field of first flux entry, H_p, into the same $Bi_2Sr_2CaCu_2O_{8+\delta}$ single crystal cut to different crystal thickness-to-width ratios (d/w), and for two angles α between the edges and the principal in-plane crystalline (a, b) axes. At all temperatures, the variation with aspect ratio of H_p is qualitatively well described by calculations for the so-called geometric barrier [E.H. Brandt, Phys. Rev. B **60**, 11939 (1999)]. However, the magnitude of H_p is strongly enhanced due to the square shape of the crystal. In the intermediate temperature regime ($T \lesssim 50$ K) in which the Bean-Livingston barrier limits vortex entry, there is some evidence for a tiny crystal-orientation dependent enhancement when the sample edges are at an angle of 45° with respect to the crystalline axes, rather than parallel to them.

PACS numbers: 74.20.rp, 74.25.Bt, 74.25.Op, 74.25.Qt

I. INTRODUCTION

Surface barriers are well-known to delay vortex penetration into high-T_c cuprates (HTSC).[1–21] As a consequence, the field of first flux penetration H_p may be significantly higher than the lower critical field $H_{c1} = \Phi_0/4\pi\mu_0\lambda^2 \ln\kappa$ (λ is the London penetration depth, $\kappa \equiv \lambda/\xi$ with ξ the coherence length, $\Phi_0 = h/2e$ is the flux quantum, and $\mu_0 = 4\pi \times 10^{-7}$ Hm^{-1}). Among possible types of barriers, the Bean–Livingston (BL) barrier[5–7,22,23] arises from the competition between the attraction of an entering vortex to the external surface (this can be described with an image vortex near the surface) and its repulsion by the screening (Meissner) current. The maximum value of the total free energy per unit length due to the introduction of a vortex, $\varepsilon_0 \ln\left(H_c/\sqrt{2}H_a\right)$, is attained when the latter is situated at a distance $\xi H_c/\sqrt{2}H_a$ from the superconductor-vacuum interface. Here, H_a is the applied magnetic field, $H_c = \sqrt{2}\kappa\varepsilon_0/\Phi_0$ is the thermodynamic critical field, and $\varepsilon_0 = \Phi_0^2/4\pi\mu_0\lambda^2$ is the vortex line energy. Therefore, for fields close to the penetration field $H_p = \sqrt{2}H_c$, the BL barrier can be overcome by thermal activation. In long thin isotropic superconductors in parallel fields, this is thought to happen by the nucleation of a vortex loop in the sample bulk.[5,6] In layered superconductors such as $Bi_2Sr_2CaCu_2O_{8+\delta}$, the vortex loop may encompass a single[7] or several pancake vortices.[6] Experiments supporting an important role of the BL barrier in HTSC are the observation of asymmetric hysteresis loops accompanied by magnetic relaxation over the barrier, near the critical temperature T_c in $YBa_2Cu_3O_{7-\delta}$,[3] and at temperatures below 50 K in layered $Tl_2Ba_2CaCu_2O_{8+\delta}$[1,2] and $Bi_2Sr_2CaCu_2O_{8+\delta}$.[4,13] Further evidence is the observation of the predicted sensitivity of the barrier to electron[4] and heavy-ion irradiation.[8,9] Namely, the presence of defects near the specimen surface perturb the screening current on the relevant length scale, larger than the coherence length ξ but smaller than λ, thereby favoring vortex nucleation.

Following theoretical predictions[24] of a possible crystal-orientation dependence of H_p in HTSC, the BL barrier has recently returned to the center of attention.[25] This orientational dependence would be due to the predominant $d_{x^2-y^2}$–symmetry of the superconducting gap in HTSC (for a review, see Ref. 26). In that case, quasiparticle scattering at surfaces oriented perpendicularly to the nodal directions give rise to Andreev bound states (ABS).[27–29] The quasi-particle current carried by these bound states is responsible for the modification of the field of first flux penetration.[24] In $Bi_2Sr_2CaCu_2O_{8+\delta}$ the relevant surfaces are those that have a normal oriented near to $\alpha = 45°$ with respect to the principal (a, b) crystalline axes.[30]

It should be noted that the BL barrier is effective only in the situation where the applied magnetic field is parallel to a large flat surface. In the opposite case of a superconducting platelet of rectangular cross-section in perpendicular magnetic field, flux entry is hindered by a barrier of geometrical origin.[10–20] The geometrical barrier comes from the competition between the line tension of a vortex cutting through the upper and lower ridges at a sample edge, and the Lorentz force due to the Meissner current. The penetration field H_p is reached when the total field at the sample equator attains H_{c1}; vortex sections penetrating from the top and the bottom ridge join, and the vortex line enters the bulk. A key experiment demonstrating the relevance of the geometrical barrier in $Bi_2Sr_2CaCu_2O_{8+\delta}$ is the measurement of the penetration field of crystals with similar aspect ratio d/w, but different shape: a prism-shaped[15,31] or ellipsoidal[32] crystal have a lower penetration field than a rectangular parallelepiped. Experiments reporting the accumulation of flux in the center of a superconductor sample immediately after first flux penetration cannot be taken as evidence for the presence of a geometrical barrier; such observations merely reflect the fact that the sample cen-

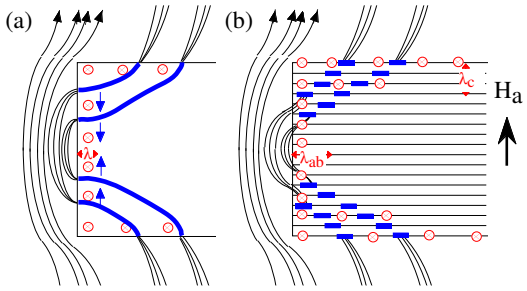

FIG. 1: (color online) Schematic diagram of vortex penetration in (a) a "continuous" superconductor in which layeredness is irrelevant and (b) in a layered superconductor; both materials are presumed to have a rectangular cross-section. Vortex lines (in blue) first penetrate at the corners, and then progress inwards to the sample equator. The direction of the screening current is indicated by the red circles. In case (a), there is no further barrier impeding the progression of the vortex lines (arrows); furthermore, the vortex currents run parallel to the lateral surface. Therefore, no effect of the Bean-Livingston barrier superimposed on that of the geometrical barrier is to be expected. In (b), the progression of the vortex line is mediated by the periodic entry of pancake vortices (blue rectangles); each of these should overcome the BL barrier. The supercurrents associated with the pancakes run in a plane perpendicular to the lateral surface, therefore the geometrical barrier is enhanced by the Bean-Livingston barrier.

ter corresponds to the location of minimal vortex free energy, a situation that stems from the macroscopic distribution of the Meissner current and is therefore true regardless of the origin of the barrier.

The flux density and current distributions accompanying vortex penetration into superconductors of rectangular cross-section and varying thickness-to-width ratio d/w was numerically calculated by Brandt.[16,17] The penetration field obtained from these calculations is well described by the formula

$$H_p = H_p^{0,\infty} \tanh\left(\sqrt{\beta d/w}\right). \qquad (1)$$

The constant β was found to be ~ 0.36 for infinite strips (bars), and ~ 0.67 for rectangular cylinders; in the absence of a BL barrier or vortex pinning, $H_p^{0,\infty} = H_{c1}$. Tentative agreement of Eq. (1) with H_p of micron-sized single crystalline $Bi_2Sr_2CaCu_2O_{8+\delta}$ was obtained for a few values of d/w and temperature T by Wang. *et al.* ,[18] while Cabral *et al.* could fit their measured hysteresis loops to those calculated in Ref. 17, but only in the temperature interval 50 – 60 K.[19]

The purpose of the present paper is twofold. In a first step, we shall verify the dependence of the field of first flux penetration in square-shaped $Bi_2Sr_2CaCu_2O_{8+\delta}$ single crystals on a wide range of aspect ratios d/w, over the entire temperature range from 20 K to T_c. This is achieved by cutting the same crystal into successively smaller squares. These measurements establish the manner by which the Bean-Livingston barrier and magnetic relaxation influence H_p, and yield the geometrical factor β for a crystal of square shape. The results are then used to verify whether any effect of crystalline orientation on Meissner screening and first flux penetration can be measured in single crystalline $Bi_2Sr_2CaCu_2O_{8+\delta}$.

The expected orientation dependence[24] should actually be largest in layered superconductors such as $Bi_2Sr_2CaCu_2O_{8+\delta}$. In thin rectangular crystals of "continuous" superconductors such as $YBa_2Cu_3O_{7-\delta}$, there is no potential barrier stopping the progression of vortex lines into the interior once the geometrical barrier is overcome (Fig. 1). Furthermore, the boundary condition imposes that the vortex current runs parallel to the crystal lateral surface. In this situation, any effect of the ABS quasi-particle current should be confined to the volume near the crystal ridges. In layered superconductors, the progression of a vortex line is mediated by the successive penetration of pancake vortices. The entry of each pancake is counteracted by a potential barrier, since the pancake currents are always in a plane perpendicular to the lateral surface. These arguments hold for HTSC as long as the applied field is not exactly parallel to the (a, b) plane, since the high crytalline anisotropy impedes vortex penetration along the c-axis. A possible contribution of ABS to the Bean-Livingston barrier in layered HTSC will come not only from the crystal ridges, but from all flat regions of the lateral surface that are oriented perpendicular to a nodal direction ($\alpha = 45°$), and all wedge-shaped regions with bisector along the nodal direction.[33] In what follows, we find a tiny enhancement of H_p for $T < 50$ K, *i.e.* , in the regime in which flux penetration is delayed by the Bean-Livingston barrier. This shows that, if any enhancement of the Bean-Livingston barrier due to ABS exists, it is either much smaller than theoretically expected, or marred by physical damage at the crystal edges. At higher temperature, no enhancement is found.

II. EXPERIMENTAL DETAILS

A rectangular $Bi_2Sr_2CaCu_2O_{8+\delta}$ single crystal is cut along its a and b axes from a seed rod grown by the travelling solvent floating zone method.[34] The crystal orientation was determined from the growth direction of the rod,[34] and verified by the precession X-ray diffraction method.[35]

Flux penetration below 80 K was imaged using direct magneto-optical imaging (MOI),[36] while for higher temperatures the Differential Magneto-Optical (DMO) method[37,38] was used. In MOI, a ferrimagnetic garnet indicator with in-plane anisotropy is placed on top of the

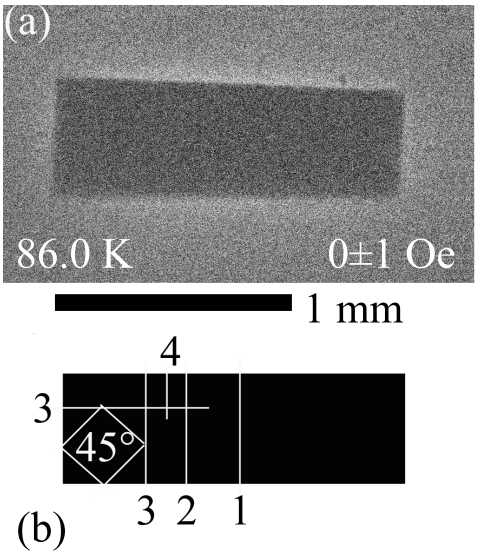

FIG. 2: (a) DMO image of Meissner screening by the initial $Bi_2Sr_2CaCu_2O_{8+\delta}$ single crystal, at 86.0 K and $H_a = 0$; the field modulation $\Delta H_a = 1$ Oe. (b) Cutting scheme. The black rectangle represents the initial crystal, white numbered lines indicate successive cuts, in order.

sample under study, and observed using a polarized light microscope. In all cases, the magnetic field, of magnitude H_a, is applied parallel to the smallest crystal dimension and the c-axis. The presence of a non-zero perpendicular component B of the magnetic induction is revealed, by virtue of the Faraday effect of the garnet, as a non-zero intensity of reflected light when the polarizers of the microscope are (nearly) crossed (see Fig. 4). Images are acquired by an automated procedure, which also ramps the magnetic field, at the same rate, $\mu_0 dH_a/dt = 5\times10^{-4}$ Ts^{-1}, for all experiments. In DMO, an image is taken at an applied field H_a; the field is then decreased to $H_a - \Delta H_a$ (with $\Delta H_a = 1$ Oe), and another image is acquired. The latter image is then subtracted from the former. The procedure is repeated 100 times, whence the 100 differential images are averaged (see Fig. 2a, and the inset to Fig. 5). The use of the DMO technique was limited to temperatures above 82 K, at which the field modulation ΔH_a is not screened once the magnetic field exceeds H_p. The field of first flux penetration was determined visually from both the direct and the differential magneto-optical images, taken at successive values of H_a, from the appearance of a non-zero B within the sample contours (Fig. 4). A more precise value could be obtained by calibrating the local intensity of the light; this yields a map of the local induction from which curves of the local magnetic hysteresis were deduced. Similar curves were obtained using a micron-sized Hall probe array.[12] Examples of these are shown in Fig. 6. The penetration field was then estimated from the peak in the hysteresis curves ($\mu_0 dH_a/dt = 1 \times 10^{-4}$ Ts^{-1} for these measurement).

In order to avoid any artefacts due to tiny variations in sample composition[39] or doping, the same $Bi_2Sr_2CaCu_2O_{8+\delta}$ crystal is chosen for all further experiments. The selected crystal, with $T_c = 88.7 \pm 0.5$K, had initial dimensions $(l = 1400) \times (w = 500) \times (d = 28)$ $\mu\mathrm{m}^3$, and was checked using the differential magneto-optical (DMO) method[37,38] to be as homogeneous as possible: macroscopic and mesoscopic inhomogeneities are known to affect H_p.[20,40] Nevertheless, some inhomogeneities arising from the crystal growth method remained.[41] Fluctuations in crystal growth rate result in small spatial variations of the composition, with a arc-shaped topology reminiscent of the floating-zone meniscus (inset of Fig. 5). The associated spatial variation of the local T_c leads to preferential flux penetration in the arc-shaped regions, above the temperatures marked by arrows in Fig. 5.

For the measurements of H_p as function of d/w, the same roughly square shape is retained to eliminate the influence of sample shape, or ambiguities related to the difference between length and width. Using a W wire saw with 1 μm SiC abrasive grains, the initial crystal, with $d/w = 0.045$, is progressively cut into five ever smaller squares, down to $d/w = 0.47$, according to the scheme of Fig. 2b. In the final step, one of the intermediate squares is cut at 45° with respect to the crystal axes; it had an aspect ratio of $d/w = 0.12$. Fig. 3 shows scanning electron micrographs of the edges obtained following the cuts. Typically, different layers of the crystal split at slightly different distances x from the crystal center, yielding an edge roughness $(\langle x^2\rangle - \langle x\rangle^2)^{1/2} \sim 2 - 3$ μm. The edges of individual layers are smooth on the scale of the penetration depth, ~ 200 nm, with occasional protrusions. The local orientation of the edge meanders about the global orientation of the crystal, with a rms deviation of 10–25°, depending on the investigated edge. No systematic morphological differences could be observed between [100] or [010] "anti-nodal" and [110] "nodal" interfaces. The crystal edges therefore seem to be suitably

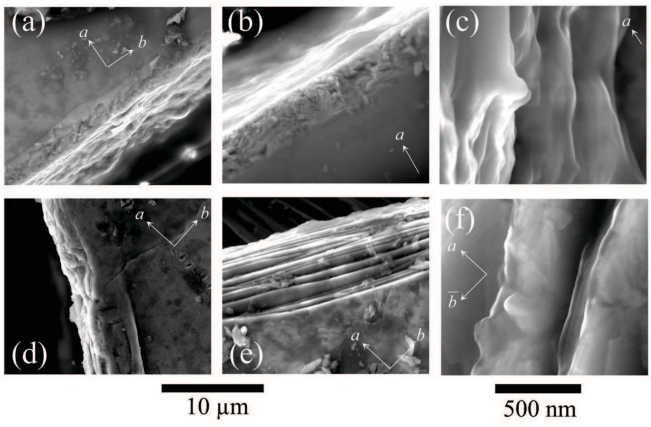

FIG. 3: Scanning electron micrographs of crystal edges cut at 90° (a-c) and at 45° with respect to the principal [100] and [010] crystal axes (d-f). Images (a,b;d,e) have the same magnification, as do images (c,f).

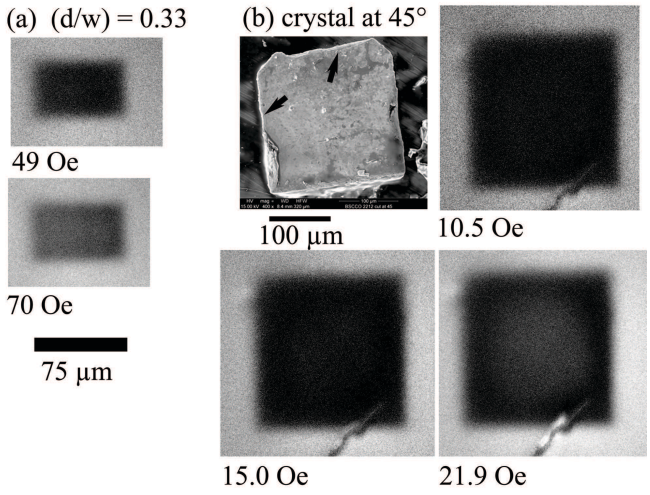

FIG. 4: (a) Flux penetration into the crystal with $d/w = 0.33$, delimited by lines "3", "3", and "2" in Fig. 2(b), at 70.0 K, and two fields below ($\mu_0 H_a = 4.9$ mT) and above ($\mu_0 H_a = 7.0$ mT) H_p, respectively. (b) Scanning electron micrograph of the crystal cut at 45°, with arrows showing the areas enlarged in Fig. 3 (d,e); the subsequent three images show flux penetration into this crystal as visualized by MOI at 80.0 K and $H_a = 10.5$ Oe $< H_p$, 15.0 Oe $\approx H_p$, as well as $H_a = 21.9$ Oe$> H_p$.

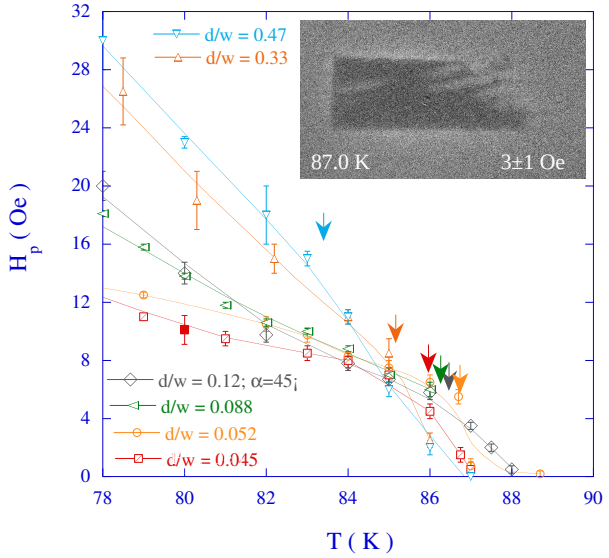

FIG. 5: (color online) Enlarged view of the penetration field data of Fig. 7 in the temperature regime close to T_c. Closed symbols denote data obtained by Hall probe magnetometry, open symbols are data measured using magneto-optical imaging. Data above 82 K are obtained using the differential magneto-optical method. Arrows show the temperature above which flux penetration is influenced by crystal inhomogeneity. For example, the inset shows flux penetration in the initial crystal of Fig. 2 ($d/w = 0.045$) at 87.0 K, measured by the DMO method at a field of 3 Oe, and a field modulation $\Delta H_a = 1$ Oe. The observed heterogeneity leads to the "collapse" of H_p at $T = 86.8$ K. Lines are guides to the eye.

described by the model advocated in Ref. 33.

III. RESULTS

The main panel of Fig. 5 shows H_p of the different crystals cut from the initial sample in the vicinity of T_c. One systematically observes a linear decrease of $H_p(T)$ upon approaching T_c, followed by a steep descent to $H_p = 0$ (see also Ref. 42). DMO imaging shows that this drop is the consequence of flux penetration into areas of lower T_c, and is therefore the hallmark of sample inhomogeneity. A similar depression of the field of first flux penetration was obtained by introducing heavy ion-irradiated regions.[40] In what follows, we shall discard data taken in the high temperature regime of inhomogeneous flux penetration.

Fig. 7 collects the penetration fields for all temperatures and all thickness/width ratios. As expected from the demagnetizing effect, the field of first flux entry strongly depends on the aspect ratio of the sample. Wide thin platelets have a lower penetration field than narrow thick ones. This shows that the local induction near the edge is mainly determined by the shape of the crystals, and that edge roughness and protrusions (Fig. 3) do not play a determining role in defining H_p. The measured dependence of H_p on d/w, presented in Fig. 8, is very well described by Eq. (1). However, the experimental values β, ranging between $\sim 2-6$ (inset to Fig. 7), are significantly larger than expected. The prefactor $H_p^{0,\infty}$ determined from the fits is presented in Fig. 9. Above $T \sim 45$ K, it corresponds to $H_{c1}(T)$ of the d-wave superconductor[43] in the limit $d/w \to \infty$, with the correct[34] zero-temperature extrapolated $H_{c1}^0(0) = 180$ Oe and $T_c = 88.7$ K as obtained from DMO. Previously attempted comparisons to the two-fluid relation,[19] $H_p^{0,\infty}(T) = H_p^{0,\infty}(0)\left[1-(T/T_c)^4\right]$ yield an anomalously low value $H_{c1}(0) \approx 100$ Oe.

We note the observation of thermally activated flux entry at all temperatures, indicative of a role of the BL barrier. In particular, the width of the hysteresis loops of Fig. 6 progressively narrows as T increases, until the loops are all but closed for $T \lesssim T_c$. As in Ref. 8, the temperature dependence of the penetration field in the regime 40 – 50 K is in qualitative agreement with the theory of Ref. 7, which has

$$H_p = \frac{H_c}{\sqrt{2}}\left(\frac{t_0+t}{\tau}\right)^{-k_B T/\varepsilon_0 s}. \qquad (2)$$

The relaxation rate is observed to be $S \sim -0.03$. However, if one attempts a quantitative fit by inserting this value, which should correspond to $S = dH_p/d\ln t \equiv k_B T/\varepsilon_0(T)s$, into Eq. (2), one obtains H_p–values that, above 50 K, fall vastly short of the measured ones. Therefore, vortex entry above this temperature is not limited by the BL barrier (see also Ref. 13). Below $T \sim 30$ K,

the shape of the hysteresis loops and the observation of remnant flux clearly indicate the effect of flux pinning. H_p shows an associated steep exponential increase as T is lowered.

The fits to Eq. (1) yield a set of master curves allowing us to assess the dependence of H_p on the relative orientation of the sample edges with respect to the principal crystal axes. For this, we present, in Fig. 9, the H_p^{45} data measured on the sample with $d/w = 0.12$, cut at 45°. These are compared to the interpolated values of H_p^0 for a hypothetical sample with the same aspect ratio, cut parallel to the principal axes ($\alpha = 0$). At temperatures above 50 K where the Bean-Livingston barrier is inoperative,[13] we find H_p^{45} to be slightly smaller than H_p^0. However, in the regime where the Bean-Livingston barrier impedes pancake vortex entry into the crystal, there is a small enhancement H_p^{45}/H_p^0 of up to about 1.25. This enhancement increases with decreasing temperature.

IV. DISCUSSION

We first discuss the enhancement of the penetration field by the BL barrier and the effect of sample shape for $\alpha = 0$. The dependence of H_p on d/w is well described by Eq. (1) at all temperatures, not only at those where the barrier is of purely geometric origin. This is a consequence of the macroscopic distribution of the Meissner current, which depends only on sample shape and the value of the penetration depth. At temperatures below 50 K, pancake vortex entry is hindered additionally by the BL barrier, which leads to a larger penetration field.[13] This enhancement is manifest through the increase of β as temperature is lowered. As temperature increases, pancake vortex penetration is accelerated due to thermal activation over the BL barrier. However, the field of first flux penetration can never drop below that of the geometrical barrier, since below this field $H < H_{c1}$ at the crystal equator and the existence of vortices in the superconductor is thermodynamically unfavorable. Once H_p is overcome, thermal activation of pancakes leads to the rapid increase of the local induction at the sample boundary to values above H_{c1}, and the concommitant closing of the magnetic hysteresis loops.

Even in the high temperature regime where the BL barrier has no effect whatsoever, the experimentally found β is much larger than that found in the calculations of Refs. 16 and 17. Such a large value of β expresses the fact that in thinner crystals, the measured penetration field is larger than what would be expected from calculations including the effect of the geometrical barrier only. An explanation is that, apart from opposing pancake entry from the side surfaces, the Bean-Livingston barrier opposes initial flux penetration across the top and bottom sample ridges, a finite size-effect that is expected to be more important for thinner crystals. Furthermore, β is enhanced because of the square shape of the sample surface perpendicular to the field direction. Although this is manifestly closer to the disk than to the strip geometry, the corners of a square superconductor are responsible for enhanced screening with respect to the disk, yielding a larger penetration field. The effect is similar to that of the ridges of a platelet of rectangular cross-section, which are responsible for additional screening

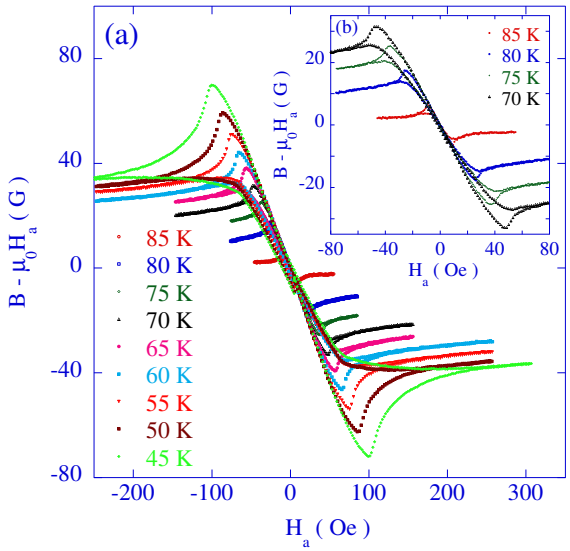

FIG. 6: (color online) Hysteresis loops of the magnetic flux density in the center of the crystal with $d/w = 0.052$, measured by a microscopic Hall probe array. The inset shows an expanded view of the loops at high temperature.

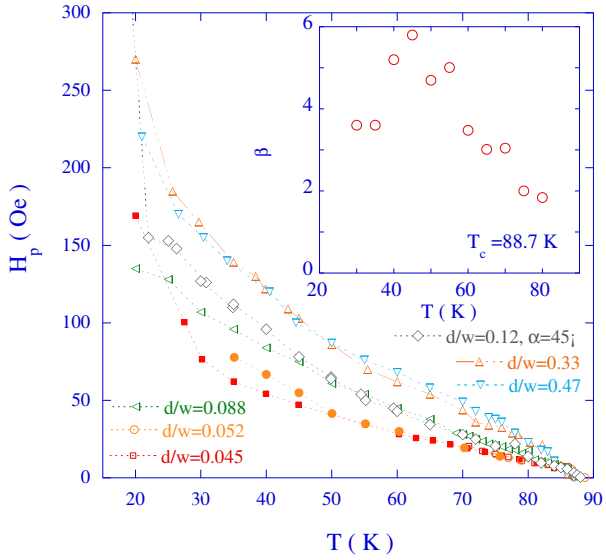

FIG. 7: (color online) The penetration field as evaluated from MO-imaging (open symbols) and Hall probe measurements (full symbols). The aspect ratio is $d/w = 0.47$, 0.33, 0.12(45°), 0.088, 0.052, 0.045, from the upper to the lower curves. The inset shows the experimentally determined factor β as function of temperature.

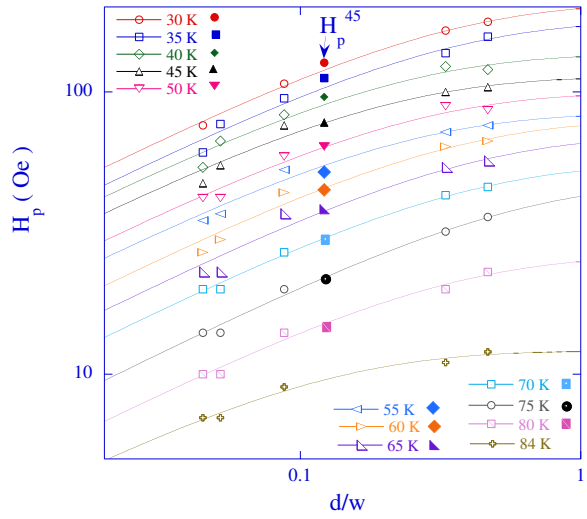

FIG. 8: (color online) Double-logarithmic plot of the penetration field of single crystalline $Bi_2Sr_2CaCu_2O_8$ as a function of aspect ratio for different temperatures. Open symbols show H_p^0 for the case where the edges are parallel to the principal axes. Drawn lines are fits to Eq. (1). Full symbols indicate H_p^{45} (edges at $\alpha = 45°$ with respect to the principal crystal axes).

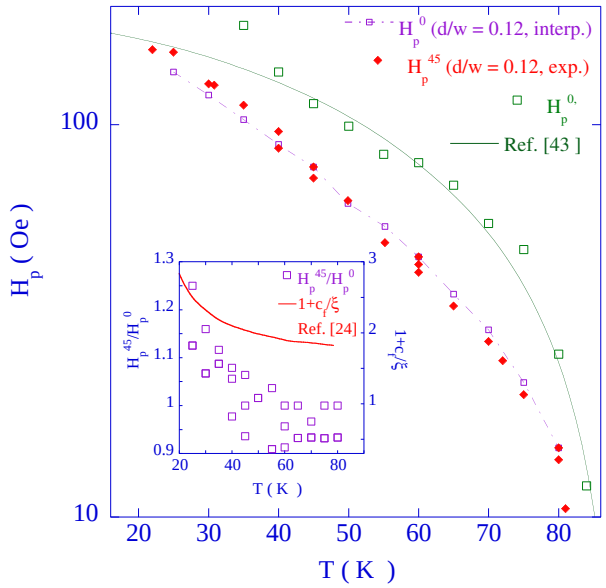

FIG. 9: (color online) Plot of the penetration field H_p^{45} of a $Bi_2Sr_2CaCu_2O_8$ crystal with the edges cut at $\alpha = 45°$ with respect to the main crystal axes (◇), compared to the interpolated values H_p^0 for a crystal with the same $d/w = 0.12$, but $\alpha = 0$ (□). Also shown is $H_p^{0\infty}(T)$ for a crystal with $d/w \to \infty$, $\alpha = 0$, extracted from the fits in Fig. 8 (□); the drawn line is a fit to the theoretical temperature dependence of H_{c1} for a d-wave superconductor,[43] with $H_{c1}(0) = 180$ Oe and $T_c = 88.7$ K. The inset shows the experimental (lefthand axis) and the theoretically expected enhancement (righthand axis) of the field of first flux penetration for $\alpha = 45°$ with respect to $\alpha = 0$.

when compared to an ellipsoidal superconductor of the same d/w. By extrapolating to T_c, at which all effects of the Bean-Livingston barrier have vanished, we find, experimentally, that $\beta \sim 1$ for a square superconductor with rectangular cross-section. Note that taking an incorrect value of β may result in large error when determining of the first critical field H_{c1} from H_p of thin superconducting platelets.

We now turn to the relative enhancement H_p^{45}/H_p^0 of the field of first flux penetration for $\alpha = 45°$, *i.e.* where the crystal edges are perpendicular to the nodal directions of the superconducting order parameter in $Bi_2Sr_2CaCu_2O_{8+\delta}$. The observation of an enhancement in the sole temperature regime where the BL barrier is relevant is in qualitative agreement with the theory of Iniotakis, Dahm, and Schopohl. The theoretically predicted enhancement $H_p^{45}/H_p^0 \sim 1 + c_f/\xi$ increases as temperature decreases (see Inset to Fig. 9). Its physical origin is that, in superconductors where the order parameter Δ undergoes a sign change on any given Fermi surface sheet, interference between quasiparticles with a relative phase difference of π will result in the occurence of Andreev bound states (ABS) on those parts of the superconductor-vacuum interface that are perpendicular, or nearly perpendicular, to the k-space direction for which Δ vanishes. For $Bi_2Sr_2CaCu_2O_{8+\delta}$ with $d_{x^2-y^2}$-wave symmetry of the order parameter,[26] these "nodal" directions correspond to $(\pm\pi, \pm\pi)$, *i.e.* at $\alpha = 45°$ with respect to the principal crystalline axes.[26] The ABS have a spatial extent of several times ξ in the direction perpendicular to the interface, and are accompanied by a local reduction of $|\Delta|$. Translational invariance along the interface allows these states to carry current. When a magnetic field is applied to the superconductor, this "anomalous" paramagnetic current adds to the diamagnetic screening current, and to the ordinary paramagnetic current resulting from the Doppler shift of quasiparticle states.[44] In the region near a nodal surface, the total Meissner current is therefore reduced with respect to surfaces that are perpendicular to the k-space direction where the gap is maximum;[45] hence, the magnetic field should penetrate somewhat further into the superconductor.[24] The presence of a vortex near the nodal interface should also affect the Andreev bound states,[46] with the result of somewhat reducing the anomalous current.[24] The BL barrier on the nodal surface must therefore be evaluated by the addition of the standard free energy contributions from the vortex-Meissner current repulsion and the attraction of the vortex to the surface; and the "anomalous" contributions arising from the extra repulsion due to the augmented field near the surface, and from the attraction between the vortex current and the bound state current.[24] The net result is an enhancement of the barrier maximum, and a shift of its location towards the bulk of the superconductor. The en-

hancement of the BL barrier should be maximum when the orientation of the superconductor-vacuum interface is perpendicular to the nodal direction (and nil when the interface is parallel to the nodal direction), and be temperature dependent. For example, at $T/T_c = 0.2$, an increase of H_p by a factor of 4 to 5 is expected on surfaces oriented at $\alpha = 45°$, with respect to the situation where $\alpha = 0$.[24]

The observation of an enhancement of H_p for the crystal with the edges cut perpendicular to the nodal directions seems to confirm the prediction by Iniotakis *et al.* of an orientation-dependent H_p due to a more important effect of Andreev bound states in this case.[24,33] The inset to Fig. 9 shows that the magnitude of the experimentally measured effect is, however, far less than predicted.[24] The prime factor that may influence the experimental result is the roughness of the edges cut by the wire saw. The undulating character of the crystal edges will entail a reduction of the local density of bound states, and should strongly diminish the total anomalous (paramagnetic) Meissner current. As for the observed wedge-shaped protrusions, recent work has shown even if the occurence of ABS depends sensitively on quasiparticle reflection at the boundary as well as the shape and precise orientation of the latter,[47] they are still expected as long as the wedge bisector is aligned close to a nodal direction.[33] However, the localised quasiparticles near to such protrusions will not contribute to the total Meissner current, and will have no effect on the Bean-Livingston barrier. In summary, the area on which the Bean-Livingston barrier is effectively enhanced is much smaller than the total area of the lateral edges. Only a fraction of pancakes composing an entering vortex line will effectively be subjected to the influence of local ABS, entailing the decrease of H_p

Finally, even in those parts of the surface where ABS would be fully developped, pancake vortices enter the crystal by thermal activation over the barrier. The implies that pancakes are nucleated at a distance that is farther removed from the edge than the predicted $\xi H_c/\sqrt{2}H_a$.[7] In Ref. 24, the magnitude and temperature dependence of the enhancement factor $1 + c_f/\xi$ strongly depends on the distance of the vortex from the crystal edge. Any enhancement of this distance due to thermal activation would imply a much smaller modification of the Meissner current, and a significant reduction of the enhancement factor.

V. CONCLUSIONS

Summarizing, we have measured the field of first flux entry, H_p, for samples of different aspect ratio and orientation, cut from the same optimally doped $Bi_2Sr_2CaCu_2O_8$ single crystal. We find that at all temperatures, the penetration field of the square–shaped crystals is satisfactorily described by Eq. (1). The numerical factor β is determined jointly by the shape of the sample surface perpendicular to the field direction and by the effect of the Bean-Livingston barrier, which, in layered superconductors, counteracts the penetration of individual pancake vortices. For the case of a square superconductor of rectangular cross-section, without the influence of a Bean-Livingston barrier, it is experimentally found that $\beta \sim 1$.

Moreover, we have investigated the enhancement of H_p when the edges are perpendicular to the nodal directions of the order parameter, *i.e.* at 45° with respect to the crystalline a and b axes. If discernible, the measured enhancement is tiny and occurs only in the temperature interval in which the Bean-Livingston barrier increases the field of first flux penetration over what would be expected from sole geometrical effects. The results are discussed in the framework of possible Andreev bound states present at the nodal surfaces of the d-wave superconductor.[24] Notably, the small value of the enhancement in comparison to theoretical prediction is ascribed to edge roughness and thermal activation of pancake vortices over the Bean-Livingston barrier.

Acknowledgements

We wish to acknowledge O. Mula, H. Martin, M. Goupil, M. Girardin, and J. Arancibia who participated in part of the work, and B. Mansart and P.A. Albouy for help with the X-ray diffraction measurement, and D. Caldemaison for the SEM micrographs. We are also indebted to E.H. Brandt, V.B. Geshkenbein, T. Shibauchi, T. Tamegai, U. Welp, and E. Zeldov for discussions.

[1] V.N. Kopylov, I.F. Shegolev, and T.G. Togonidze, Physica (Amsterdam) C **162**–**164**, 1143 (1989).
[2] V.N. Kopylov, A.E. Koshelev, I.F. Shegolev, and T.G. Togonidze, Physica (Amsterdam) C **170**, 291 (1990).
[3] M. Konczykowski, L.I. Burlachkov, Y.Yeshurun, and F. Holtzberg, Phys. Rev. B **43**, 13707 (1991); M. Konczykowski, in *Critical Current Limitations in High Temperature Superconductors* , ed. M. Baran, W. Gorzkowski, and H. Szymczak (World Scientific, 1991).
[4] N. Chikumoto, M. Konczykowski, N. Motohira, and A.P. Malozemoff, Phys. Rev. Lett. **69**, 1260 (1992).
[5] L. Burlachkov, Phys. Rev. B **47**, 8056 (1993).
[6] A.E. Koshelev, Physica (Amsterdam) C **191**, 219 (1992); A.E. Koshelev, Physica (Amsterdam) C **223**, 276 (1994).
[7] L. Burlachkov, V.B. Geshkenbein, A.E. Koshelev, A.I. Larkin, and V.M. Vinokur, Phys. Rev. B **50**, 16770 (1994).
[8] J.K. Gregory, M.S. James, S.J. Bending, C.J. van der Beek, and M. Konczykowski, Phys. Rev. B**64**, 134517 (2001).

[9] A.E. Koshelev and V.M. Vinokur, Phys. Rev. B **64**, 134518 (2001)

[10] M.V. Indenbom, G. D' Anna, M.-O. André, W. Benoit, H. Kronmüller, T.W. Li, and P.H. Kes, in *Proceedings of the* 7$^{\text{th}}$ *Int. Workshop on Critical Currents in Superconductors* , Alpbach, Austria, Jan. 24–27, 1994, Edited by H.W. Weber (World Scientific, 1994).

[11] M.V. Indenbom, A. Forkl, B. Ludescher, H. Kronmüller, H.-U. Habermeier, B. Leibold, G. D'Anna, T.W. Li, P.H. Kes, A.A. Menovsky, Physica C **226**, 325 (1994).

[12] E. Zeldov, A.I. Larkin, V.B. Geshkenbein, M. Konczykowski, D. Majer, B. Khaykovich, V.M. Vinokur, and H. Shtrikman, Phys. Rev. Lett. **73**, 1428 (1994).

[13] E. Zeldov, D. Majer, M. Konczykowski, A.I. Larkin, V.M. Vinokur, V.B. Geshkenbein, N. Chikumoto, and H. Shtrikman, Europhys. Lett. **30**, 367 (1995).

[14] M. Benkraouda and J.R. Clem, Phys. Rev. B **53**, 5716 (1996).

[15] N. Morozov, E. Zeldov, M. Konczykowski, and R.A. Doyle, Physica (Amsterdam) C **291**, 113 (1997).

[16] E.H. Brandt, Phys. Rev. B **60**, 11939 (1999).

[17] E.H. Brandt, J. Low. Temp. Phys. **27**, 723 (2001).

[18] Y.M. Wang, A. Zettl, S. Ooi, and T. Tamegai, Phys. Rev. B **65**, 184506 (2002).

[19] L.R.E. Cabral, C.C. de Souza Silva, J.A. Aguiar, and E.H. Brandt, Phys. Rev. B **65**, 134514 (2002).

[20] M.R. Connolly, M.V. Milošević, S.J. Bending, and T. Tamegai, Phys. Rev. B **78**, 132501 (2008).

[21] J.R. Clem, Journal of Superconductivity and Novel Magnetism **6**, 1557 (2008).

[22] P.G. de Gennes, *Superconductivity of Metals and Alloys* , pp. 76-79 , W.A. Benjamin (New York, 1966).

[23] C.P. Bean and J.D. Livingston, Phys. Rev. Lett. **12**, 14 (1964).

[24] C. Iniotakis, T. Dahm, and N. Schopohl, Phys. Rev. Lett. **100**, 037002 (2008).

[25] G. Leibovitch, R. Beck, A. Kohen, G. Deutscher, arXiv:0901.1774v1 (2009).

[26] C.C. Tsuei et J.R. Kirtley, Rev. Mod. Phys. **72**, 969 (2000).

[27] C.R. Hu, Phys. Rev. Lett. **72**, 1526 (1994).

[28] Y. Tanaka and S. Kashiwaya, Phys. Rev. Lett. **74**, 3451 (1995).

[29] S. Kashiwaya and Y. Tanaka, Rep. Prog. Phys. **63**, 1641 (2000).

[30] J.R. Kirtley, C.C. Tsuei, H. Raffy, Z.Z. Li, A. Gupta, J.Z. Sun, S. Megtert, Europhysics Lett. **36**, 707 (1996).

[31] T.B. Doyle, R. Labusch, and R.A. Doyle, Physica (Amsterdam) C **290,** 148 (1997).

[32] R.A. Doyle, S.F.W.R. Rycroft, C.W. Dewhurst, E. Zeldov, I. Tsabba, S. Reich, T.B. Doyle, T. Tamegai, and S. Ooi, Physica (Amsterdam) C **308**, 123 (1998).

[33] C. Iniotakis, Physica (Amsterdam) C **460-462**, 1143 (2007).

[34] Ming Li, C.J. van der Beek, M. Konczykowski, A.A. Menovsky, and P.H. Kes, Phys. Rev. **66**, 024502 (2002).

[35] M.J. Buerger, *The photography of the reciprocal lattice* , AXSRED Monograph **1**, Cambridge (Ma.) 1944.

[36] L.A. Dorosinskiĭ, M.V.Indenbom, V.I. Nikitenko, Yu.A. Ossip'yan, A.A. Polyanskii, and V.K. Vlasko-Vlasov, Physica C **203**, 149 (1992).

[37] A. Soibel, E. Zeldov, M.L. Rappaport, Y. Myasoedov, T. Tamegai, S. Ooi, M. Konczykowski, and V. Geshkenbein, Nature **406**, 282 (2000).

[38] A. Soibel, Y. Myasoedov, M.L. Rappaport, T. Tamegai, S.S. Banerjee, and E. Zeldov, Phys. Rev. Lett. **87**, 167001 (2001).

[39] T.W. Li, P.H. Kes, N.T. Hien, J.J.M. Franse, and A.A. Menovsky, J. Cryst. Growth **135**, 481 (1994).

[40] N. Avraham, E.H. Brandt, G.P. Mikitik, Y. Myasoedov, M. Rappaport, E. Zeldov, C.J. van der Beek, M. Konczykowski, and T. Tamegai, Phys. Rev. B **77**, 214525 (2008).

[41] M. Yasugaki, M. Tokunaga, N. Kameda, and T. Tamegai, Phys. Rev. B **67**, 104504 (2003).

[42] The steep drop in H_p was previously erroneously interpretd as being due to the effect of vortex fluctuations, see D.A. Brawner, A. Schilling, H.R. Ott, R.J. Haug, K. Ploog, and K. von Klitzing, Phys. Rev. Lett. **71**, 785 (1993).

[43] R.J. Radtke, V.N. Kostur, and K. Levin, Phys. Rev. B **53**, R522 (1996).

[44] M. Tinkham, *Introduction to Superconductivity*[R.E. Krieger Publ. Company, Malabar, Florida (1980)], p 59 vv.

[45] M. Fogelstrom, D. Rainer, and J.A. Sauls, Phys. Rev. Lett. **79**, 281 (1997).

[46] S. Graser, C. Iniotakis, T. Dahm, and N. Schopohl, Phys. Rev. Lett. **93**, 247001 (2004).

[47] C. Iniotakis, S. Graser, T. Dahm, and N. Schopohl, Phys. Rev. B **71**, 214508 (2005).